

ANALYTICAL AND NUMERICAL ANALYSIS OF INJECTION PUMP (STEPPED) SHAFT VIBRATIONS USING TIMOSHENKO THEORY

Stanisław NOGA^{*}, Edward REJMAN^{**}, Paweł BAŁON^{***},
Bartłomiej KIEŁBASA^{***}, Robert SMUSZ^{**}, Janusz SZOSTAK^{***}

^{*}Rzeszów University of Technology, Al. Powstańców Warszawy 12, 35 – 959 Rzeszów, Poland

^{**}ZPU Mirosław Pogoda, ul. Wojska Polskiego 3, 39 – 300 Mielec, Poland

^{***}AGH University of Science and Technology, WIMiR, Al. A. Mickiewicza 30-B2, 30-059 Kraków, Poland

noga@prz.edu.pl, erejman@prz.edu.pl, balonpawel@gmail.com,
bartek.kielbasa@gmail.com, robmsusz@gmail.com, szostak@agh.edu.pl

received 29 March 2022, revised 5 May 2022, accepted 12 May 2022

Abstract: The free transverse vibrations of shafts with complex geometry are studied using analytical methods and numerical simulations. A methodology is proposed for evaluating the results of a natural transverse vibration analysis as generated by finite element (FE) models of a shaft with compound geometry. The effectiveness of the suggested approach is tested using an arbitrarily chosen model of the injection pump shaft. The required analytical models of the transverse vibrations of stepped shafts are derived based on the Timoshenko thick beam theory. The separation of variables method is used to find the needed solutions to the free vibrations. The eigenvalue problem is formulated and solved by using the FE representation for the shaft and for each shaft-simplified model. The results for these models are discussed and compared. Additionally, the usefulness of the Myklestad–Prohl (MP) method in the field of preliminary analysis of transverse vibration of complex shaft systems is indicated. It is important to note that the solutions proposed in this paper could be useful for engineers dealing with the dynamics of various types of machine shafts with low values of operating speeds.

Key words: modal analysis, natural vibrations, analytical solutions, Timoshenko beam theory, shaft vibrations

1. INTRODUCTION

The progress of modern engineering requires the use of advanced tools in the field of computer-aided design and computer-aided engineering calculations at the design stage. This applies in particular to devices, assemblies and their individual elements, all of which are required to have adequate durability and reliability during operation. Such important components of devices include, among others, machine shafts [1]. One of the essential factors, which could disturb or limit the functioning of devices (e.g., pumps and others), is the vibration of the components or assemblies of these systems [1,2]. The rapid growth of computer techniques and analytical systems based on the finite element method (FEM) allows a free vibration analysis of the complex design and geometry systems to be conducted [1]. In paper [3], FEM was used to analyse lateral vibrations of the drilling rig. Cases of the system with and without damping were analysed. In paper [4], transversal vibration of a low-power electrical rotor is studied using FEM and other analytical and numerical methods. Based on the developed finite element (FE) models, the basic dynamic parameters of the analysed system are determined. FEM modelling is used in paper [5] to analyse transverse vibrations of a Timoshenko beam with an elastic foundation composed of two different regions of the Winkler type. The developed FE models were used to determine the frequencies for which there are no harmonic type of free vibrations. An important aspect is the ability to verify the developed FE

models of the designed systems. In the case of newly designed systems, conducting laboratory tests must have a strong economic justification. Therefore, it seems justified to conduct research allowing for the development of FE model verification methods with the lowest possible economic cost. The monograph by Friswell and Mottershead [6] discusses the theoretical foundations and practical applications of techniques for obtaining numerical FE models consistent with the model data in the accepted frequency range (the so-called model updating methods). Cases where reference data are obtained from analytical solutions of vibrating systems and from measurement experiments were considered. It is also worth mentioning monograph [1], in which theoretical and experimental issues concerning vibrations of systems, and the consideration of modern measuring tools and computer techniques are discussed. In works [4,5,7], the results of analytical solutions (natural frequency values) were used as reference data to verify the proposed FE models of discussed systems. A spectral element model for a spinning uniform shaft was developed in paper [8], and FEM analysis was used for evaluating the accuracy of the proposed model through some example problems. Shahgholi et al. [9] discussed the issues of transverse vibrations of a slender shaft using analytical methods. In the modelling of the studied system, the rotary inertia and gyroscopic effect are considered. Many studies use the results of theoretical analysis based on the Timoshenko beam vibration theory as a source of reference data. It is worth mentioning that the Timoshenko beam theory allows one to obtain a model that considers all important

physical phenomena in one-dimensional continuous systems [2,10]. The fundamental vibration theory of the thick (Timoshenko) beam is presented in several monographs [2, 10]. In the monograph of Noga [7], one can find an extension of the Timoshenko theory into ring systems with an elastic foundation. In paper [11], the influence of the two-parameter elastic soil on the dynamic behaviour of the Timoshenko beam with a variable cross-section was examined in the presence of conservative axial loads, and the needed theoretical issues were concisely presented in matrix form. In paper [12], the description and solution of the Timoshenko beam free and forced vibrations by using a single equation are proposed. Analysis was carried out for various cases of the boundary conditions. In article [13], exact frequencies and mode shapes were calculated for the Timoshenko beam on different boundary supports and partially loaded with a distributed mass span. They agree with the experimental data. In article [14], the authors effectively developed the Timoshenko theory for the vibration problem of the beam with functionally graded properties along their thickness. In papers [15, 16], the free vibration behaviours of a functionally graded disk-shaft rotor system reinforced with graphene nanoplatelets resting on elastic supports are investigated. In both mentioned works, equations of motion including the gyroscopic effect due to rotation are derived by employing the Lagrange formalism within the framework of Timoshenko beam theory for the shaft and Kirchhoff plate theory for the disk. Additionally, in article [16], the disk-shaft rotor with eccentric mass was included in the investigation. In contrast, in papers [17, 18], the free vibration of a rotating, functionally graded pre-twisted blades-shaft assembly reinforced with graphene nanoplatelets was analytically investigated based on the proposed coupled model. In these papers, the governing equations of motion are derived by using the Lagrange equation within the framework of the Rayleigh beam theory and Euler-Bernoulli beam theory. The work in paper [17] refers to the pre-twisted blade-shaft system, while paper [18] refers to the pre-twisted double blade-shaft system. In paper [19], the authors studied the influence of von Kármán nonlinearity on the values of frequency, thermoelastic damping and quality factors on Timoshenko beam resonators based on the modified couple stress theory. Another research field is the issue of vibrations of composite shafts. In work [20], the Bernoulli-Euler beam theory is used to achieve the exact solution for the vibration of a cross-ply laminated composite drive shaft with an intermediate joint. The joint is modelled as a frictionless internal hinge. In paper [21], a new multi-layer FE, dedicated for dynamic analysis of rotating laminated shafts, is formulated and based on layerwise and shaft theories. Another approach found in the literature on the subject concerns transfer matrix methods, where one of them is the Myklestad-Prohl (MP) method. The idea and usefulness of the MP method in the analysis of transverse vibrations of shafts were presented for the first time in paper [22]. The MP method was effectively used in paper [4] to analyse the transverse vibrations of the shaft of a low-power electric engine. In article [23], the extended transfer matrix method dedicated to the analysis of the torsion- and flexure-coupled vibration of a damped multi-degree-of-freedom shafting system subjected to external excitations is utilized. In work [24], the modification of the transfer matrix method was developed for the analysis of bending vibrations of the steel composite transmission shafting system. The needed relations were obtained based on the lamination theory and the layerwise beam theory. The achieved results were successfully verified by experimental data and FEM. In paper [25], the flexural vibration of Timoshenko beams using a distributed lumped modelling tech-

nique are discussed. Two types of elements are discussed: the so-called distributed elements (dedicated to parts of shafts with a distributed mass) and lumped elements (dedicated to parts of shafts with a concentrated mass). The obtained results are successfully verified using other techniques. In article [26], the approach was expanded for analysis of compound shafts, considering the gyroscopic effect. The proposed technique was effectively employed by the authors for a multistep gas turbine rotor system. This paper continues the authors' research [4,5,7] related to analytical modelling, FEM simulations and model quality evaluation techniques of compound mechanical systems.

The present paper deals with transverse vibrations of a shaft of complex geometry. Analytical methods and numerical simulations were used during studies. The novel methodology for evaluation of results of free transverse vibration analysis as generated by the FE models of shafts with complex geometry is presented. The required analytical models of the transverse vibrations of stepped shafts are developed based on the Timoshenko theory. Finally, the concluding remarks are made and the adequate natural forms of vibrations referring to the appropriate natural frequencies of the systems are shown.

2. FORMULATION OF THE PROBLEM

This article discusses the vibration problem of dedicated stepped shafts which operate in injection pumps. As can be seen in Fig. 1, the shaft has a compound stepped shaft arrangement. Additionally, the shaft is hollow within a certain portion of its length. This geometric shape is due to the specific structure of the injection pump. Because of the proprietary nature of the assembly construction, the specifications of the shaft are not given. Due to its complexity and usually lower values of the natural frequency [1,2,10], the case of bending vibrations of the shaft will be analysed.

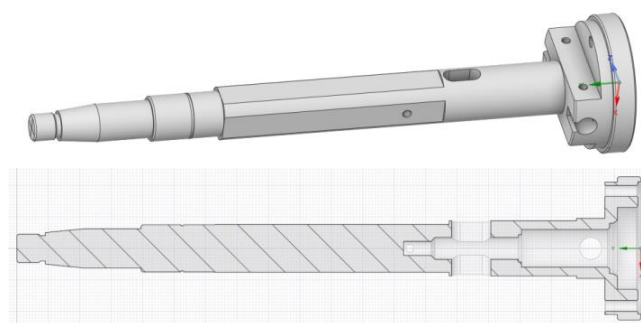


Fig. 1. Geometrical model of the system under consideration

The main goal of this work is to develop a reliable methodology for evaluating the results of natural transverse vibration analyses in the assumed frequency range as generated by the developed FE model of the pertinent shaft. It would be a more preferable situation to have the results of the experimental research of the shaft, but at the conceptual and design stage, access to this type of data is typically unrealistic. Therefore, the following methodology for evaluating the results of the natural vibration analyses generated from the elaborated FE model of the object is proposed. Based on the generated FE model of the system and for the arbitrarily chosen boundary conditions determine the values of

the natural frequencies of bending vibrations and the corresponding normal modes in the assumed frequency range. Then, a stepped shaft model (the simplified model) with simplified geometry should be developed, for which it is possible to derive analytical equations of bending free vibrations. Because the considered system does not meet the criterion of the technical theory of thin beam vibrations (the so-called Bernoulli beam theory) [2,10], therefore, while developing the equations of free vibrations, the Timoshenko beam theory (the so-called thick beam theory) will be used [2,10]. Then, for the adopted, simplified model, the FE model solution and the exact solution of the analytical model are developed, and for the previously set boundary conditions, the natural frequencies and the corresponding vibration natural forms are determined. Achieved from the simplified model, the results (which come from the analytical solutions and FEM simulation) are compared with the results received from the discussed shaft FE model and if necessary, the simplified model is modified to obtain satisfactory compliance of the results in terms of the adopted criterion.

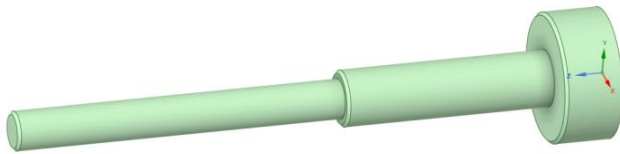


Fig. 2. Geometrical model of the three-stepped simplified shaft

In this paper, it will be shown that satisfactory results can be obtained for the discussed shaft, assuming that the simplified shaft is a three-stepped hollow shaft (see Fig. 2). In addition, the results of the FE model of the discussed system shaft will be verified with a model developed based on the MP method [22]. The considerations presented in this paper are performed under the assumption that the boundary conditions imposed on the analysed systems correspond to the conditions of a cantilever beam. Because of the specific geometry of the discussed models (see Figs. 1–5 and Tab. 1) and the relatively low value of the operating speed (<1,500 rpm), the centrifugal and gyroscopic effects of the shaft are omitted. In the authors' humble opinion, the proposed methodology will be useful for engineers dealing with the transverse vibration analysis of systems of such type, especially at the design stage.

3. THEORETICAL FORMULATION

The subject of the considerations is a stepped shaft, treated as a Timoshenko beam, with continuous segments. It is assumed that the beam has three compartments and in the individual compartments it is homogeneous with a circular-symmetric cross-section. Little vibration with no damping is considered. The vibration equation of the Timoshenko beam with the continuous segments can be written as follows [2,10]:

$$\begin{aligned}
 &-\frac{\partial}{\partial x} \left(\kappa A_i G \left(\frac{\partial w_i}{\partial x} - \phi_i \right) \right) + \rho A_i \frac{\partial^2 w_i}{\partial t^2} = 0 \\
 &-\frac{\partial}{\partial x} \left(E I_i \frac{\partial \phi_i}{\partial x} \right) - \kappa A_i G \left(\frac{\partial w_i}{\partial x} - \phi_i \right) + \rho I_i \frac{\partial^2 \phi_i}{\partial t^2} = 0
 \end{aligned} \quad (1)$$

where $w_i = w_i(x, t)$ is the transverse beam displacement, $\phi_i = \phi_i(x, t)$ is the rotation of the beam cross section,

x and t are the coordinate and the time, κ is the shear correction factor, l_1, l_2 and l_3 are the beam dimensions, A_1, A_2 and A_3 are the cross-sectional areas of the corresponding compartments of the beam, I_1, I_2 and I_3 are the area moments of inertia of cross sections of the appropriate compartments of the beam, ρ is the mass density, E is the Young's modulus of elasticity and G is the modulus of elasticity in shear (i.e., Kirchhoff's modulus). In Eq. (1), $i = 1$ for $0 \leq x \leq l_1$, $i = 2$ for $l_1 \leq x \leq l_1 + l_2$ and $i = 3$ for $l_1 + l_2 \leq x \leq l_1 + l_2 + l_3$.

For the cantilever beam case, the appropriate boundary conditions are as follows [2,10]:

$$\begin{aligned}
 w_1(0, t) = 0, \quad \phi_1(0, t) = 0, \quad \frac{\partial \phi_3(l_1+l_2+l_3, t)}{\partial x} = 0, \\
 \frac{\partial w_3(l_1+l_2+l_3, t)}{\partial x} - \phi_3(l_1 + l_2 + l_3, t) = 0.
 \end{aligned} \quad (2)$$

In the boundary sections of homogeneous compartments of the beam, the compatibility conditions provide the following groups of equations [2,10], i.e., for $x = l_1$:

$$\begin{aligned}
 w_1(l_1, t) = w_2(l_1, t), \quad \phi_1(l_1, t) = \\
 \phi_2(l_1, t), \quad E I_1 \frac{\partial \phi_1(l_1, t)}{\partial x} = E I_2 \frac{\partial \phi_2(l_1, t)}{\partial x}, \\
 \kappa A_1 G \left(\frac{\partial w_1(l_1, t)}{\partial x} - \phi_1(l_1, t) \right) = \kappa A_2 G \left(\frac{\partial w_2(l_1, t)}{\partial x} - \phi_2(l_1, t) \right).
 \end{aligned} \quad (3)$$

and for $x = l_1 + l_2$:

$$\begin{aligned}
 w_2(l_1 + l_2, t) = w_3(l_1 + l_2, t), \quad \phi_2(l_1 + l_2, t) = \\
 \phi_3(l_1 + l_2, t), \\
 E I_2 \frac{\partial \phi_2(l_1+l_2, t)}{\partial x} = E I_3 \frac{\partial \phi_3(l_1+l_2, t)}{\partial x}, \\
 \kappa A_2 G \left(\frac{\partial w_2(l_1+l_2, t)}{\partial x} - \phi_2(l_1 + l_2, t) \right) = \kappa A_3 G \left(\frac{\partial w_3(l_1+l_2, t)}{\partial x} - \phi_3(l_1 + l_2, t) \right).
 \end{aligned} \quad (4)$$

The first two relations in Eqs (3) and (4) are the continuity conditions and the last two are the equilibrium conditions, respectively.

4. FREE VIBRATION ANALYSIS

The objective of this section is to determine an analytical solution for the free vibration of the discussed system. To solve the system Eq. (1), the Bernoulli–Fourier method (separation of variables) can be used. So, the general solution to Eq. (1) takes the following form [2,10]:

$$\begin{aligned}
 w_i(x, t) = W_i(x)T(t), \quad \phi_i(x, t) = F_i(x)T(t), \\
 T(t) = A \cos(\omega t) + B \sin(\omega t), \quad i = 1,2,3
 \end{aligned} \quad (5)$$

where ω is the circular frequency of the discussed system vibration. After introducing solution (5) to Eq. (1) it can produce the following equation:

$$\begin{aligned}
 W_i''(x) + a_0 W_i(x) - F_i'(x) = 0, \\
 F_i''(x) + b_i W_i'(x) - c_0 F_i'(x) = 0, \quad i = 1,2,3
 \end{aligned} \quad (6)$$

where

$$a_0 = \omega^2 \frac{\rho}{\kappa G}, \quad b_i = \frac{\kappa A_i G}{E I_i}, \quad c_i = \omega^2 \frac{\rho}{E} - \frac{\kappa A_i G}{E I_i}, \quad i = 1,2,3 \quad (7)$$

and the prime refers to the derivative of the function to x . By eliminating the function $F_i(x)$ ($i = 1,2,3$) from Eq. (6), one can get equations for transverse displacements $W_1(x), W_2(x)$ and $W_3(x)$ in the following form:

$$\begin{aligned} W_1^{(IV)}(x) + (a_0 + b_1 + c_1)W_1''(x) + a_0c_1W_1(x) &= 0 \\ W_2^{(IV)}(x) + (a_0 + b_2 + c_2)W_2''(x) + a_0c_2W_2(x) &= 0 \\ W_3^{(IV)}(x) + (a_0 + b_3 + c_3)W_3''(x) + a_0c_3W_3(x) &= 0 \end{aligned} \quad (8)$$

The boundary conditions (2) in terms of $W_i(x)$ take the following form:

$$\begin{aligned} W_1(0) = 0, \quad W_1'''(0) + (a_0 + b_1)W_1'(0) &= 0, \\ W_3''(l_1 + l_2 + l_3) + a_0W_3(l_1 + l_2 + l_3) &= 0, \\ W_3'''(l_1 + l_2 + l_3) + (a_0 + b_3 + c_3)W_3'(l_1 + l_2 + l_3) &= 0 \end{aligned} \quad (9)$$

And accordingly, the compatibility conditions (3) and (4) at $x = l_1$ in terms of $W_i(x)$ become:

$$\begin{aligned} W_1(l_1) = W_2(l_1), \quad \frac{1}{c_1}[W_1'''(l_1) + (a_0 + b_1)W_1'(l_1)] &= \\ \frac{1}{c_2}[W_2'''(l_1) + (a_0 + b_2)W_2'(l_1)], \quad EI_1[W_1''(l_1) + & \\ a_0W_1(l_1)] = EI_2[W_2''(l_1) + a_0W_2(l_1)], & \quad (10) \\ \kappa A_1 G[W_1'''(l_1) + (a_0 + b_1 + c_1)W_1'(l_1)] = & \\ \kappa A_2 G[W_2'''(l_1) + (a_0 + b_2 + c_2)W_2'(l_1)] & \end{aligned}$$

and at $x = l_1 + l_2$ they take the following form:

$$\begin{aligned} W_2(l_1 + l_2) = W_3(l_1 + l_2), \\ \frac{1}{c_2}[W_2'''(l_1 + l_2) + (a_0 + b_2)W_2'(l_1 + l_2)] &= \\ = \frac{1}{c_3}[W_3'''(l_1 + l_2) + (a_0 + b_3)W_3'(l_1 + l_2)], & \quad (11) \\ EI_2[W_2''(l_1 + l_2) + a_0W_2(l_1 + l_2)] &= \\ = EI_3[W_3''(l_1 + l_2) + a_0W_3(l_1 + l_2)], & \\ \kappa A_2 G[W_2'''(l_1 + l_2) + (a_0 + b_2 + c_2)W_2'(l_1 + l_2)] = & \\ \kappa A_3 G[W_3'''(l_1 + l_2) + (a_0 + b_3 + c_3)W_3'(l_1 + l_2)] & \end{aligned}$$

$$T_1 = \begin{bmatrix} \cos(\lambda_{11}l_1) & \sin(\lambda_{11}l_1) & \cosh(\lambda_{12}l_1) & \sinh(\lambda_{12}l_1) \\ c_2m21_1 \sin(\lambda_{11}l_1) & c_2m22_1 \cos(\lambda_{11}l_1) & c_2m2_1 \sinh(\lambda_{12}l_1) & c_2m2_1 \cosh(\lambda_{12}l_1) \\ m31_1 \cos(\lambda_{11}l_1) & m31_1 \sin(\lambda_{11}l_1) & m32_1 \cosh(\lambda_{12}l_1) & m32_1 \sinh(\lambda_{12}l_1) \\ m41_1 \sin(\lambda_{11}l_1) & m42_1 \cos(\lambda_{11}l_1) & m4_1 \sinh(\lambda_{12}l_1) & m4_1 \cosh(\lambda_{12}l_1) \end{bmatrix} \quad (17)$$

$$T_{21} = \begin{bmatrix} \cos(\lambda_{21}l_1) & \sin(\lambda_{21}l_1) & \cosh(\lambda_{22}l_1) & \sinh(\lambda_{22}l_1) \\ c_1m21_2 \sin(\lambda_{21}l_1) & c_1m22_2 \cos(\lambda_{21}l_1) & c_1m2_2 \sinh(\lambda_{22}l_1) & c_1m2_2 \cosh(\lambda_{22}l_1) \\ m31_2 \cos(\lambda_{21}l_1) & m31_2 \sin(\lambda_{21}l_1) & m32_2 \cosh(\lambda_{22}l_1) & m32_2 \sinh(\lambda_{22}l_1) \\ m41_2 \sin(\lambda_{21}l_1) & m42_2 \cos(\lambda_{21}l_1) & m4_2 \sinh(\lambda_{22}l_1) & m4_2 \cosh(\lambda_{22}l_1) \end{bmatrix} \quad (18)$$

$$T_{22} = \begin{bmatrix} \cos(\lambda_{21}l_{12}) & \sin(\lambda_{21}l_{12}) & \cosh(\lambda_{22}l_{12}) & \sinh(\lambda_{22}l_{12}) \\ c_3m21_2 \sin(\lambda_{21}l_{12}) & c_3m22_2 \cos(\lambda_{21}l_{12}) & c_3m2_2 \sinh(\lambda_{22}l_{12}) & c_3m2_2 \cosh(\lambda_{22}l_{12}) \\ m31_2 \cos(\lambda_{21}l_{12}) & m31_2 \sin(\lambda_{21}l_{12}) & m32_2 \cosh(\lambda_{22}l_{12}) & m32_2 \sinh(\lambda_{22}l_{12}) \\ m41_2 \sin(\lambda_{21}l_{12}) & m42_2 \cos(\lambda_{21}l_{12}) & m4_2 \sinh(\lambda_{22}l_{12}) & m4_2 \cosh(\lambda_{22}l_{12}) \end{bmatrix}, \quad l_{12} = l_1 + l_2 \quad (19)$$

$$T_3 = \begin{bmatrix} \cos(\lambda_{31}l_{12}) & \sin(\lambda_{31}l_{12}) & \cosh(\lambda_{32}l_{12}) & \sinh(\lambda_{32}l_{12}) \\ c_2m21_3 \sin(\lambda_{31}l_{12}) & c_2m22_3 \cos(\lambda_{31}l_{12}) & c_2m2_3 \sinh(\lambda_{32}l_{12}) & c_2m2_3 \cosh(\lambda_{32}l_{12}) \\ m31_3 \cos(\lambda_{31}l_{12}) & m31_3 \sin(\lambda_{31}l_{12}) & m32_3 \cosh(\lambda_{32}l_{12}) & m32_3 \sinh(\lambda_{32}l_{12}) \\ m41_3 \sin(\lambda_{31}l_{12}) & m42_3 \cos(\lambda_{31}l_{12}) & m4_3 \sinh(\lambda_{32}l_{12}) & m4_3 \cosh(\lambda_{32}l_{12}) \end{bmatrix}, \quad l_{12} = l_1 + l_2 \quad (20)$$

and

$$\begin{aligned} m21_i = \lambda_{i1}^3 - (a_0 + b_i)\lambda_{i1}, \quad m31_i = I_i(-\lambda_{i1}^2 + a_0), \\ m41_i = A_i(\lambda_{i1}^3 - (a_0 + b_i + c_i)\lambda_{i1}), \\ m22_i = -\lambda_{i1}^3 + (a_0 + b_i)\lambda_{i1}, \quad m32_i = I_i(\lambda_{i2}^2 + a_0), \\ m42_i = A_i(-\lambda_{i1}^3 + (a_0 + b_i + c_i)\lambda_{i1}), \\ m2_i = \lambda_{i2}^3 + (a_0 + b_i)\lambda_{i2}, \quad i = 1,2,3, \\ m4_i = A_i(\lambda_{i2}^3 + (a_0 + b_i + c_i)\lambda_{i2}) \end{aligned} \quad (21)$$

As in paper [13], the boundary conditions can be written as follows:

In this article, the case where the natural frequencies are below the critical value is analysed. It gives the following restrictions on the value of the frequency range:

$$\omega^2 < \frac{\kappa A_i G}{\rho I_i}, \quad i = 1,2,3 \quad (12)$$

Conditions (12) guarantee the harmonic type of free vibration. The general solution for the discussed case can be written as [2,10]:

$$W_i(x) = D_{i1} \cos(\lambda_{i1}x) + D_{i2} \sin(\lambda_{i1}x) + D_{i3} \cosh(\lambda_{i2}x) + D_{i4} \sinh(\lambda_{i2}x), \quad i = 1,2,3 \quad (13)$$

where

$$2\lambda_{i1}^2 = \alpha + \sqrt{\gamma^2 + \eta_i}, \quad 2\lambda_{i2}^2 = -\alpha + \sqrt{\gamma^2 + \eta_i}, \quad i = 1,2,3 \quad (14)$$

and

$$\alpha = \omega^2 \rho \left(\frac{1}{\kappa G} + \frac{1}{E} \right), \quad \gamma = \omega^2 \rho \left(\frac{1}{E} - \frac{1}{\kappa G} \right), \quad \eta_i = \frac{4\omega^2 \rho A_i}{EI_i}, \quad i = 1,2,3 \quad (15)$$

Substituting Eq. (13) into Eqs (10) and (11), the following matrix equations are obtained:

$$T_1 \begin{bmatrix} D_{11} \\ D_{12} \\ D_{13} \\ D_{14} \end{bmatrix} = T_{21} \begin{bmatrix} D_{21} \\ D_{22} \\ D_{23} \\ D_{24} \end{bmatrix} \text{ and } T_{22} \begin{bmatrix} D_{21} \\ D_{22} \\ D_{23} \\ D_{24} \end{bmatrix} = T_3 \begin{bmatrix} D_{31} \\ D_{32} \\ D_{33} \\ D_{34} \end{bmatrix} \quad (16)$$

where

$$T_1 = \begin{bmatrix} \cos(\lambda_{11}l_1) & \sin(\lambda_{11}l_1) & \cosh(\lambda_{12}l_1) & \sinh(\lambda_{12}l_1) \\ c_2m21_1 \sin(\lambda_{11}l_1) & c_2m22_1 \cos(\lambda_{11}l_1) & c_2m2_1 \sinh(\lambda_{12}l_1) & c_2m2_1 \cosh(\lambda_{12}l_1) \\ m31_1 \cos(\lambda_{11}l_1) & m31_1 \sin(\lambda_{11}l_1) & m32_1 \cosh(\lambda_{12}l_1) & m32_1 \sinh(\lambda_{12}l_1) \\ m41_1 \sin(\lambda_{11}l_1) & m42_1 \cos(\lambda_{11}l_1) & m4_1 \sinh(\lambda_{12}l_1) & m4_1 \cosh(\lambda_{12}l_1) \end{bmatrix} \quad (17)$$

$$T_{21} = \begin{bmatrix} \cos(\lambda_{21}l_1) & \sin(\lambda_{21}l_1) & \cosh(\lambda_{22}l_1) & \sinh(\lambda_{22}l_1) \\ c_1m21_2 \sin(\lambda_{21}l_1) & c_1m22_2 \cos(\lambda_{21}l_1) & c_1m2_2 \sinh(\lambda_{22}l_1) & c_1m2_2 \cosh(\lambda_{22}l_1) \\ m31_2 \cos(\lambda_{21}l_1) & m31_2 \sin(\lambda_{21}l_1) & m32_2 \cosh(\lambda_{22}l_1) & m32_2 \sinh(\lambda_{22}l_1) \\ m41_2 \sin(\lambda_{21}l_1) & m42_2 \cos(\lambda_{21}l_1) & m4_2 \sinh(\lambda_{22}l_1) & m4_2 \cosh(\lambda_{22}l_1) \end{bmatrix} \quad (18)$$

$$T_{22} = \begin{bmatrix} \cos(\lambda_{21}l_{12}) & \sin(\lambda_{21}l_{12}) & \cosh(\lambda_{22}l_{12}) & \sinh(\lambda_{22}l_{12}) \\ c_3m21_2 \sin(\lambda_{21}l_{12}) & c_3m22_2 \cos(\lambda_{21}l_{12}) & c_3m2_2 \sinh(\lambda_{22}l_{12}) & c_3m2_2 \cosh(\lambda_{22}l_{12}) \\ m31_2 \cos(\lambda_{21}l_{12}) & m31_2 \sin(\lambda_{21}l_{12}) & m32_2 \cosh(\lambda_{22}l_{12}) & m32_2 \sinh(\lambda_{22}l_{12}) \\ m41_2 \sin(\lambda_{21}l_{12}) & m42_2 \cos(\lambda_{21}l_{12}) & m4_2 \sinh(\lambda_{22}l_{12}) & m4_2 \cosh(\lambda_{22}l_{12}) \end{bmatrix}, \quad l_{12} = l_1 + l_2 \quad (19)$$

$$T_3 = \begin{bmatrix} \cos(\lambda_{31}l_{12}) & \sin(\lambda_{31}l_{12}) & \cosh(\lambda_{32}l_{12}) & \sinh(\lambda_{32}l_{12}) \\ c_2m21_3 \sin(\lambda_{31}l_{12}) & c_2m22_3 \cos(\lambda_{31}l_{12}) & c_2m2_3 \sinh(\lambda_{32}l_{12}) & c_2m2_3 \cosh(\lambda_{32}l_{12}) \\ m31_3 \cos(\lambda_{31}l_{12}) & m31_3 \sin(\lambda_{31}l_{12}) & m32_3 \cosh(\lambda_{32}l_{12}) & m32_3 \sinh(\lambda_{32}l_{12}) \\ m41_3 \sin(\lambda_{31}l_{12}) & m42_3 \cos(\lambda_{31}l_{12}) & m4_3 \sinh(\lambda_{32}l_{12}) & m4_3 \cosh(\lambda_{32}l_{12}) \end{bmatrix}, \quad l_{12} = l_1 + l_2 \quad (20)$$

$$K_1 \begin{bmatrix} D_{11} \\ D_{12} \\ D_{13} \\ D_{14} \end{bmatrix} + K_3 \begin{bmatrix} D_{31} \\ D_{32} \\ D_{33} \\ D_{34} \end{bmatrix} = 0 \quad (22)$$

where

$$K_1 = \begin{bmatrix} 1 & 0 & 1 & 0 \\ 0 & m22_1 & 0 & m21_1 \\ 0 & 0 & 0 & 0 \\ 0 & 0 & 0 & 0 \end{bmatrix} \quad (23)$$

$$K_3 = \begin{bmatrix} 0 & 0 & 0 & 0 \\ 0 & 0 & 0 & 0 \\ \frac{m_{313}}{I_3} \cos(\lambda_{31} l_{13}) & \frac{m_{313}}{I_3} \sin(\lambda_{31} l_{13}) & \frac{m_{323}}{I_3} \cosh(\lambda_{32} l_{13}) & \frac{m_{323}}{I_3} \sinh(\lambda_{32} l_{13}) \\ \frac{m_{413}}{A_3} \sin(\lambda_{31} l_{13}) & \frac{m_{423}}{A_3} \cos(\lambda_{31} l_{13}) & \frac{m_{43}}{A_3} \sinh(\lambda_{32} l_{13}) & \frac{m_{43}}{A_3} \cosh(\lambda_{32} l_{13}) \end{bmatrix}, \quad l_{13} = l_1 + l_2 + l_3 \quad (24)$$

Using Eq. (16), the coefficient vectors $[D_{11} D_{12} D_{13} D_{14}]^T$ and $[D_{21} D_{22} D_{23} D_{24}]^T$ can be eliminated to give:

$$\begin{bmatrix} D_{11} \\ D_{12} \\ D_{13} \\ D_{14} \end{bmatrix} = T_1^{-1} T_{21} T_{22}^{-1} T_3 \begin{bmatrix} D_{31} \\ D_{32} \\ D_{33} \\ D_{34} \end{bmatrix} \quad (25)$$

and the boundary condition (22) can be written in the matrix form:

$$[K_1 T_1^{-1} T_{21} T_{22}^{-1} T_3 + K_3] \begin{bmatrix} D_{31} \\ D_{32} \\ D_{33} \\ D_{34} \end{bmatrix} = 0 \quad (26)$$

The determinant equation in the natural frequencies is obtained from the condition of nontrivial solution. It yields the secular determinant:

$$|K_1 T_1^{-1} T_{21} T_{22}^{-1} T_3 + K_3| = 0 \quad (27)$$

where the roots of the determinant Eq. (27) $\omega = \omega_n$, ($n = 1, 2, 3, \dots$) are the exact natural frequencies. The corresponding eigenvectors of Eq. (26) together with Eq. (16) determine the eigenfunctions in terms of Eq. (13). The eigenfunctions give the normal modes of the cantilever stepped Timoshenko beam.

5. MYKLESTAD-PROHL METHOD ANALYSIS

A relatively convenient method of determining the natural frequency and the corresponding normal modes of shafts and beams is the MP numerical method [22]. In the initial assumption, it consists of the value of the natural frequency sought, and checking whether this value meets the adopted boundary conditions. If not, the calculations are repeated for the next value. The shaft (or beam) is divided into the so-called calculation points, located at the contact points of homogeneous sections of the stepped shaft (or beam). At each k – the calculation point, the following quantities are determined: shaft (beam) transverse displacement Y_k , deflection angle ψ_k , bending moment M_k and shear force T_k , according to the following equation [22]:

$$\begin{aligned} Y_{k+1} &= Y_k + z_{k+1} \psi_k + \frac{z_{k+1}^2}{2EI_{k+1}} M_k + \frac{z_{k+1}^3}{6EI_{k+1}} T_k, \\ \psi_{k+1} &= \psi_k + \frac{z_{k+1}}{EI_{k+1}} M_k + \frac{z_{k+1}^2}{2EI_{k+1}} T_k, \\ M_{k+1} &= M_k + z_{k+1} T_k, \\ T_{k+1} &= T_k + m_{k+1} \omega^2 z_{k+1}. \end{aligned} \quad (28)$$

where z_{k+1} is the distance between points k and $k + 1$, I_{k+1} is the area moment of inertia of the cross section of the shaft (beam) between points k and $k + 1$, E is the aforementioned earlier Young's modulus, m_k is the discrete mass in k -th point and ω is the assumed natural frequency. Boundary conditions for the discussed calculation case (cantilever beam) take the following form:

$$Y_0 = 0, \quad \psi_0 = 0, \quad M_{k_0} = 0, \quad T_{k_0} = 0 \quad (29)$$

where k_0 is the final calculation point. More information on the MP method can be found in reference [22].

6. FE REPRESENTATIONS

In this section the FE models of the discussed systems are formulated. The free vibration of each of the achieved discrete models (FE models of discussed objects) is described by the set of independent (decoupled) differential equations, cast in modal generalised coordinates through the use of the normal modes of the system [1]. The solution to the independent modal equations is superimposed to obtain the response of the system. To determine the eigenpairs (eigenvalue and eigenvector) related to the natural frequencies and corresponding normal modes of the discussed systems, the block Lanczos method is used [1]. The elaborated FE models are treated as approximations of the analytical models of the considered systems (especially the stepped simplified shafts).

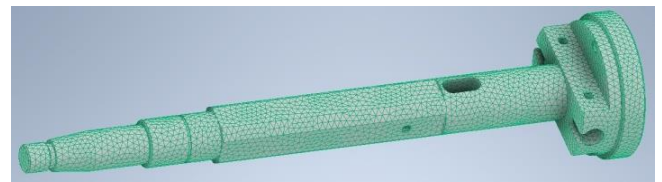


Fig. 3. FE model of the system under consideration

The modelling and analysis process are conducted using the ANSYS WORKBENCH software. To obtain models with the optimal number of elements, the surfaces resulting from the softening of feather edges are ignored in the geometrical models. This is addressed specifically for the model of the considered shaft. During the mesh generation process of the discussed systems, the 10-node tetrahedral element, with three degrees of freedom in each node, is applied. Moreover, it is assumed that the maximum length of the FE side in each model is ≤ 3.5 mm. The prepared model of the discussed shaft is shown in Fig. 3 and it includes 52,777 solid elements. The primary geometric dimensions of the accepted simplified stepped shaft (diameters: $(D_1, D_2, D_3, d_1, d_2, d_3)$ lengths: (l_1, l_2, l_3)) are shown in Fig. 4, and were partially taken from the considered system.

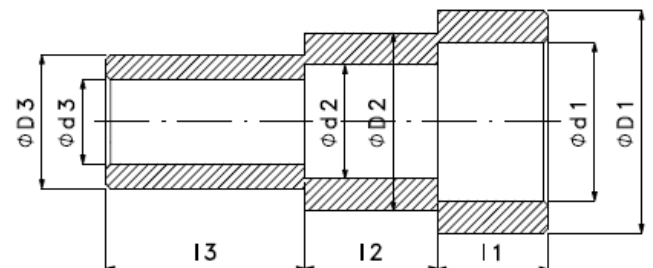


Fig. 4. Geometric dimensions of the three-stepped simplified shaft

The simplified stepped shaft FE models are prepared according to the same rules as those used with the FE model of the

discussed shaft. The two FE models of the simplified stepped shaft were developed with slight dimensional differences. The first FE model includes 32,871 FEs and the second model includes 36,158 elements. The prepared FE simplified models are shown in Fig. 5.

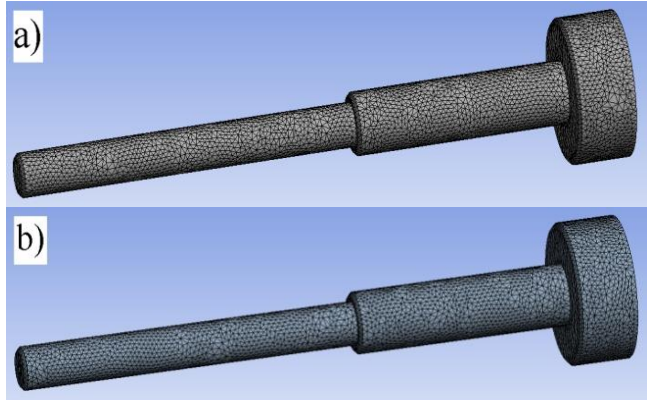


Fig. 5. FE models of the simplified stepped shaft: (a) the first model and (b) the second model

For each model case, the boundary conditions were assumed as for a cantilever beam, fixing the end of the shaft with a larger diameter. The difference between the discussed models is defined as follows [6]:

$$\varepsilon = (\omega^f - \omega^e) / \omega^e \cdot 100\% \quad (30)$$

where ω^f and ω^e are the natural frequencies of the approximate and reference models, respectively. Eq. (30) is the so-called frequency error [6]. As will be shown later, there is a significant similarity in the shape of the respective normal modes of individual models. For this reason, the similarity measure due to the normal modes (Modal Assurance Criterion (MAC indicator)) is not used.

7. NUMERICAL ANALYSIS

Numerical solutions for free vibrations analysis of the systems considered earlier are determined. This section of the study discusses and compares only the first six natural frequencies and mode shapes for transverse types of vibrations. As mentioned earlier, it is not possible to disclose the dimensions of the system under consideration, while the geometric dimensions of the three simplified stepped shafts are given in Tab. 1 and the needed technical data are given in Tab. 2. According to the theory [1,2,10], it should be expected that the normal modes of the transverse vibrations of the considered systems will occur within two perpendicular planes. In these considerations, the results of the vibration analysis of the pump shaft's FE model (see Fig. 3) are used as the reference data.

As the considered shaft does not show circular symmetry, one should expect the occurrence of slight differences in the shape of the same normal modes and in the values of the corresponding natural frequencies in the perpendicular planes mentioned. Fig. 6 shows how the vibration planes are set, where the first vibration plane is the plane shown in Fig. 6a, and the second vibration plane is the plane shown in Fig. 6b.

Tab. 1. Parameters characterising the simplified stepped shafts (see Fig. 4)

No. of the model	D_1 (mm)	D_2 (mm)	D_3 (mm)	d_1 (mm)	d_2 (mm)	d_3 (mm)	l_1 (mm)	l_2 (mm)	l_3 (mm)
1	85	37	26	29	20	0	38	139	220
2	85	37	26	27	18	4	38	139	220

Tab. 2. Technical data of the systems under study

E (Pa)	ρ (kg/m ³)	ν	κ
$2 \cdot 10^{11}$	7,850	0.3	0.9

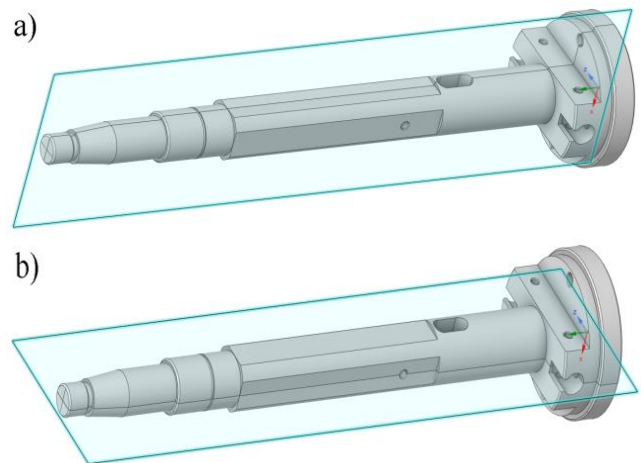


Fig. 6. Planes of transverse vibration: (a) the first plane and (b) the second plane

For example, the term transverse vibration in the first plane should be understood to mean that the potential induced transverse displacement may take place in the vertical plane, shown in Fig. 6a, while when speaking of the transverse vibration in the second plane, it is understood that it is the transverse movement in the horizontal plane shown in Fig. 6b. Tab. 3 shows the values of the natural frequencies of the shaft under consideration obtained from the FEM simulation. In the second row of Tab. 3, the frequency values refer to the vibration modes in the first plane, and the frequency values from the third row refer to the vibration modes in the second plane. When analysing the obtained results, there are slight differences in the frequency values related to individual normal modes. As mentioned earlier, the results in Tab. 3 are taken as reference data. A visualization of the relevant mode shapes is included in the Fig. 7, 12

Tab. 3. Natural frequencies of the studied shaft (FEM solution)

No. of frequencies (n)	1	2	3	4	5	6
ω_n (Hz)	199.50	1,135.49	2,747.01	4,879.47	7,504.79	10,304.44
	213.57	1,133.79	2,809.93	5,150.03	7,533.49	10,016.96

FEM, finite element method.

Tab. 4 presents the values of the natural frequencies obtained from the FEM simulation of two FE models of the three simplified stepped shafts and their respective frequency errors (30). Due to their geometry, simplified models are circularly symmetric systems. When analysing the obtained results, it can be seen that in relation to the frequency ω_1 in both cases of simplified models, the compliance of the frequency value with the value of the natural frequency of the discussed system relating to the natural form of vibrations in the second plane is better (<5%). In both the model cases, for the frequency ω_2 there is a frequency error >10%. Thus, it is generally disadvantageous. In other cases, the frequency error has absolute values of $\leq 7\%$. In general, it can be concluded that the obtained results are satisfactory and there is a significant dynamic similarity of the proposed simplified models with the reference model in terms of the adopted criterion (the frequency error (30)).

Tab. 4. Result of simulation for the auxiliary models (FEM solution)

n						
No. of auxiliary models	1	2	3	4	5	6
Natural frequencies of the first auxiliary model ω_n (Hz)						
1	219.98	984.15	2,619. 2	4,929. 0	7,370. 7	10,692
	220.00	984.26	2,619. 3	4,929. 4	7,371. 0	10,692
Natural frequencies of the second auxiliary model ω_n (Hz)						
2	226.01	995.2	2,623. 7	4,945. 2	7,397. 1	10,704
	226.01	995.3	2,624. 0	4,945. 5	7,397. 5	10,704
Frequency error of the auxiliary models ϵ_n (%)						
1	10.26	-13.33	-4.65	1.02	-1.79	3.76
	3.01	-13.19	-6.78	-4.28	-2.16	6.74
2	13.28	-12.36	-4.49	1.35	-1.44	3.88
	5.83	-12.21	-6.62	-3.97	-1.81	6.86

FEM, finite element method.

Tab. 5 presents the values of the natural frequencies obtained from the analytical solution of secular Eq. (27) relating to two models of the three stepped simplified shafts (the first four rows). The last four rows in Tab. 5 contain frequency errors (30) resulting from a comparison of the results of analytical solutions (27) with the results of the FEM simulation of the discussed system (see Tab. 3). When analysing the obtained results, it is noticed that in both cases of simplified models, for the frequency ω_2 , there is a frequency error with an absolute value >19%, so it is, of course, disadvantageous, but in other cases, the frequency error takes absolute values <7.2%. One subject of further research will be to determine why there are a relatively large absolute values of the frequency error only for the frequency ω_2 . In general, it can be concluded that the obtained results are more satisfactory as in the previous case (see Tab. 4) and there is a significant dynamic similarity between the proposed simplified analytical models (stepped Timoshenko beams) and the reference model in terms of the adopted criterion (the frequency error (30)).

Tab. 5. Result of simulation for the auxiliary models (analytical solutions)

n						
No. of auxiliary models	1	2	3	4	5	6
Natural frequencies of the first auxiliary model ω_n (Hz)						
1	198.57	896.46	2,841. 6	4,838. 5	7,362. 2	1,0286
	198.57	896.46	2,841. 6	4,838. 5	7,362. 2	1,0286
Natural frequencies of the second auxiliary model ω_n (Hz)						
2	206.16	914.51	2,830. 6	4,807. 3	7,353. 6	1,0195
	206.16	914.51	2,830. 6	4,807. 3	7,353. 6	1,0195
Frequency error of the auxiliary models ϵ_n (%)						
1	-0.47	-21.05	3.44	-0.84	-1.9	-0.18
	-7.02	-20.93	1.13	-6.05	-2.27	2.69
2	3.33	-19.46	3.04	-1.48	-2.02	-1.06
	-3.47	-19.34	0.74	-6.66	-2.39	1.78

In Tab. 6 the values of the frequency errors come from comparison of the results of analytical solutions (27), with the results of the FEM simulation of the auxiliary models (simplified stepped shaft models) shown. In this case, the results of analytical solutions (27) of the auxiliary models were taken as reference data. When analysing the obtained results, it is noticed that in relation to the first simplified model for the first natural frequency (ω_1) the frequency error is slightly >10%, for the second natural frequency (ω_2) the frequency error is $\leq 10\%$. For the remaining frequencies, the frequency error in absolute terms is <7.5%. In the case of the second simplified model, for the first two frequencies, the frequency error is slightly >9%, and for the remaining frequencies, the frequency error absolute value is <7%. With regard to the second simplified model, the FEM solution shows better compliance in terms of the adopted criterion with the analytical solution compared with the results obtained for the first simplified model. Overall, it can be said that the results presented in Tab. 6 are satisfactory.

Tab. 6. Evaluation of the quality of the auxiliary models (analytical and FEM solutions)

n						
No. of auxiliary models	1	2	3	4	5	6
Frequency error of the first auxiliary model ϵ_n (%)						
1	10.78	9.78	-7.83	1.87	0.12	3.95
	10.79	9.79	-7.82	1.88	0.12	3.95
Frequency error of the second auxiliary model ϵ_n (%)						
2	9.63	8.82	-7.31	2.87	0.59	4.99
	9.63	8.83	-7.3	2.88	0.6	4.99

FEM, finite element method

The results in Tab. 7 concern the comparison of the results obtained from the MP method with the results achieved from the FE model of the discussed system. In this case as before, the results obtained from the FE model of the discussed system (see Tab. 3) are taken as reference data. When developing the MP model of the shaft, the system was divided into 28 sections with lengths ranging from 10 mm to 20 mm, thus obtaining 29 calculation points. The required mass values at calculation points and the area moments of inertia of individual sections between the points were determined using the Autodesk Inventor environment. As in the previous cases, the boundary conditions were assumed as for a cantilever beam (Eq. 29). Relevant calculations were made in accordance with Eqs (28) and (29). As the considered shaft is not a circular-symmetric system, it should be expected that the transverse vibrations will take place in the first and second planes (Fig. 6). For this reason, it was necessary to develop two MP models, taking into account the above-mentioned planes of possible movement. In the computational process, the values of the moments of inertia were modified in a certain group of intervals and the obtained results are summarized in Tab. 7. The last two rows in Tab. 7 contain frequency errors (30) resulting from the comparison of the results of MP models solutions (28) with the results of the FEM simulation of the discussed system (see Tab. 3). The first MP model shows a satisfactory agreement with the reference model in terms of the adopted criterion (for each natural frequency, the absolute value of the frequency error is <8.21%). In the second MP model, for the frequency ω_6 there is a frequency error with the absolute value of 14.9%, which is unfavourable. The frequency errors for the remaining natural frequencies of the second MP model are at an acceptable level of value. Overall, it can be said that the results presented in Tab. 7 are satisfactory.

Tab. 7. Results of simulation by using Myklestad–Prohl models

n						
No. of models	1	2	3	4	5	6
Natural frequencies of the proposed MP models ω_n (Hz)						
1	200.7 5	1,157. 2	2,824. 8	5,027. 8	7,997. 5	1,1225
2	213.5	1,182. 4	2,928. 7	5,301. 0	8,342. 5	1,1660
Frequency error of the MP models ε_n (%)						
1	-0.62	-1.88	-2.75	-2.95	-6.16	-8.20
2	0.03	-4.11	-4.06	-2.85	-9.70	-14.9

MP, Myklestad–Prohl

Summarizing the presented results, a satisfactory compliance of the proposed simplified models and the Myklestad–Prohl models with the FE model of the analysed shaft in terms of the adopted criterion is noticed. Satisfactory compliance with the analytical models is particularly important. The obtained results confirm the correctness of the proposed verification strategy for FE models of machine shaft type systems.

Graphical visualization of the mode shapes of the system under study can be seen below (Fig 7, 8, 9, 10, 11, 12).

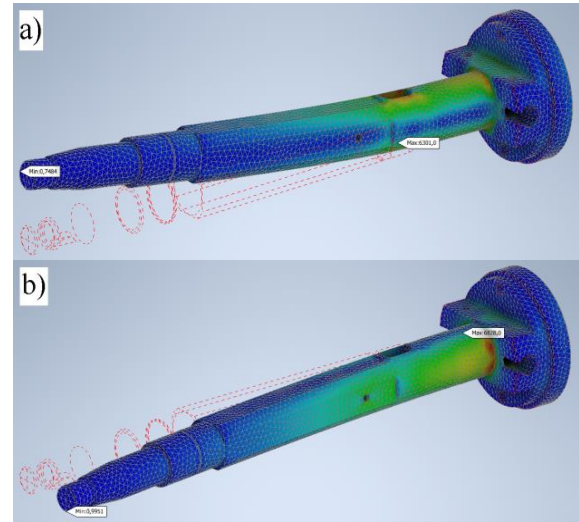


Fig. 7. Mode shapes related to the frequency ω_1 : (a) the first vibration plane and (b) the second vibration plane

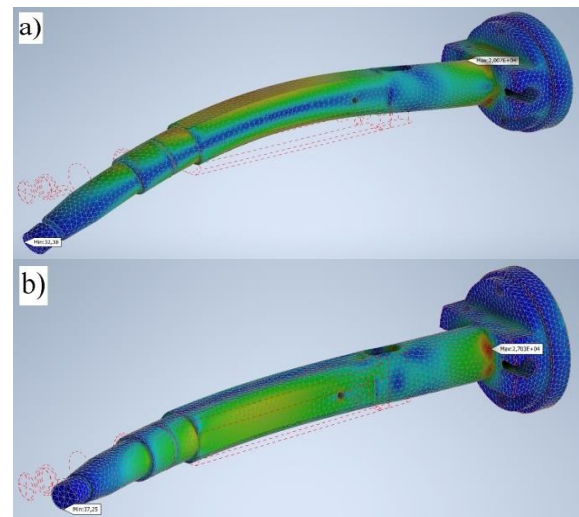


Fig. 8. Mode shapes related to the frequency ω_2 : (a) the first vibration plane and (b) the second vibration plane

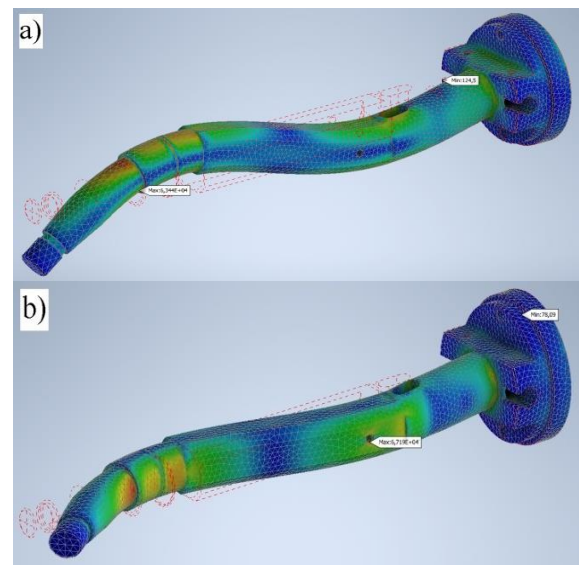


Fig. 9. Mode shapes related to the frequency ω_3 : (a) the first vibration plane and (b) the second vibration plane

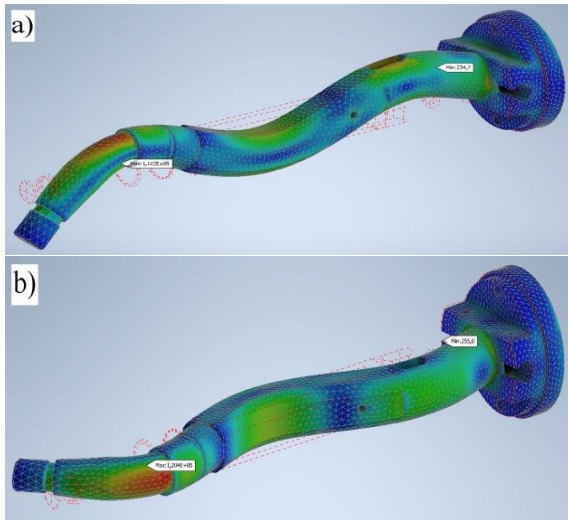


Fig. 10. Mode shapes related to the frequency ω_4 : (a) the first vibration plane and (b) the second vibration plane

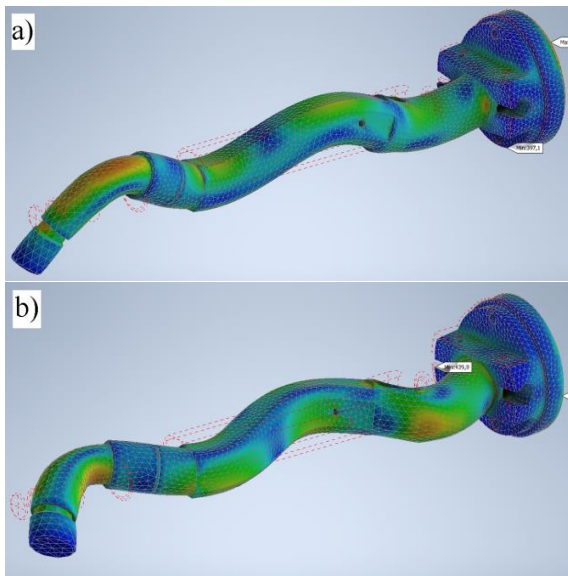


Fig. 11. Mode shapes related to the frequency ω_5 : (a) the first vibration plane and (b) the second vibration plane

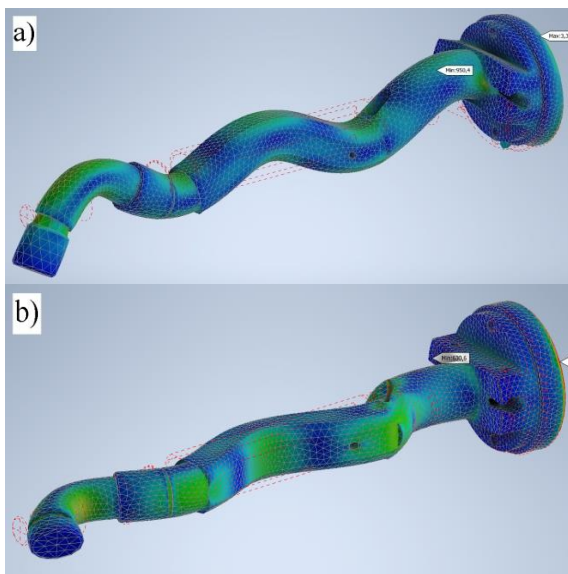


Fig. 12. Mode shapes related to the frequency ω_6 : (a) the first vibration plane and (b) the second vibration plane

8. SUMMARY

This paper presents the studies of the free transverse vibrations of shafts with compound geometry using analytical and numerical methods. The methodology for evaluating the results of the natural vibration analysis generated from the FE model of the shaft is proposed. The required analytical models of the transverse vibrations of the stepped shafts were developed based on the Timoshenko beam theory. Needed analytical solutions of the free vibrations of the discussed system are determined by using the separation of variables method. The effectiveness of the suggested approach is tested by using the selected geometrical model of the shaft dedicated to work in an injection pump. The analytical solutions are compared with the corresponding FEM solutions. The proposed analytical and numerical models give satisfactory results for a wide range of frequencies. It is remarkable how the analytical approach reduces the calculation time and computer memory requirements, and computing power when compared with the FEM solutions. The obtained results of the analysis indicate the usefulness of the MP method in the field of preliminary analysis of transverse vibrations of shaft-type systems with complex geometry. Considering the achieved results, it can be stated that when structures are analysed at their initial stage of development, simplified calculation models can be used for preliminary estimates of dynamic parameters of interest to the user. These models make it possible to pre-define the order of magnitude of the dynamic parameters of the tested objects of interest and provide some information on the quality of FEM solutions. The method proposed herein may be useful for dynamic analysis of systems such as various types of machine shafts.

REFERENCES

1. de Silva C. Vibration and Shock Handbook. Taylor & Francis. Boca Raton. 2005.
2. Rao SS, Vibration of Continuous Systems. Wiley. Hoboken. 2007.
3. Ngo VT, Xie D, Xiong Y, Zhang H, Yang Y. Dynamic analysis of a rig shafting vibration based on finite element. *Frontiers of Mechanical Engineering*. 2013;8:244-251.
4. Noga S. Dynamical analysis of the low – power electrical engine rotor. 10 European Mechanics of Materials Conference (EMMC10). Kazimierz Dolny. June 11-14. 2017:457-465.
5. Noga S, Bogacz R. Free vibration of the Timoshenko beam interacting with the Winkler foundation. *Symulacja w Badaniach i Rozwoju*. 2011;2(4):209-223.
6. Friswell M, Mottershead J. Finite Element Model Updating in Structural Dynamics. Kluwer Academic Publishers. Dordrecht. 1995.
7. Noga S. Analytical and Numerical Problems of Systems with Circular Symmetry Vibrations. Publishing House of Rzeszow University of Technology. Rzeszow. Poland (in Polish). 2015.
8. Lee U, Jang I. Spectral element model for the vibration of a spinning Timoshenko shaft. *Journal of Mechanics of Materials and Structures*. 2012;7(2):145-164.
9. Shahgholi M, Khadem SE, Bab S. Free vibration analysis of a non-linear slender rotating shaft with simply support conditions. *Mechanism and Machine Theory*. 2014;82:128-140.
10. Kaliski S. Vibration and Waves in Solids. IPPT PAN. Warsaw (in Polish). 1966.
11. Auciello NM. Vibrations of Timoshenko beams on two parameter elastic soil. *Engineering Transactions*. 2008; 56(3):187-200.
12. Majkut L. Free and forced vibrations of Timoshenko beams described by single difference equation. *Journal of Theoretical and Applied Mechanics*. 2009;47(1):193-210.

13. Chan KT, Wang XQ. Free vibration of a Timoshenko beam partially loaded with distributed mass. *Journal of Sound and Vibration*. 1997;206:353-369.
14. Awrejcewicz J, Krysko AV, Pavlov SP, Zhigalov MV, Krysko VA. Chaotic dynamics of size dependent Timoshenko beams with functionally graded properties along their thickness. *Mechanical Systems and Signal Processing*. 2017;93:415-430.
15. Zhao TY, Cui YS, Pan HG, Yuan HQ, Yang J. Free vibration analysis of a functionally graded graphene nanoplatelet reinforced disk-shaft assembly with whirl motion. *International Journal of Mechanical Sciences*. 2021;197:106335.
16. Zhao TY, Cui YS, Wang YQ, Pan HG. Vibration characteristics of graphene nanoplatelet reinforced disk-shaft rotor with eccentric mass. *Mechanics of Advanced Materials and Structures*. 2021. <https://doi.org/10.1080/15376494.2021.1904525>.
17. Zhao TY, Jiang LP, Pan HG, Yang J, Kitipornchai S. Coupled free vibration of a functionally graded pre-twisted blade-shaft system reinforced with graphene nanoplatelets. *Composite Structures*. 2021; 262:113362.
18. Zhao TY, Jiang LP, Yu YX, Wang YQ. Study on theoretical modeling and mechanical performance of a spinning porous graphene nanoplatelet reinforced beam attached with double blades. *Mechanics of Advanced Materials and Structures*. <https://doi.org/10.1080/15376494.2022.2035862>; 2022.
19. Awrejcewicz J, Krysko VA, Pavlov SP, Zhigalov MV, Kalutsky LA, Krysko VA. Thermoelastic vibrations of a Timoshenko microbeam based on the modified couple stress theory. *Nonlinear Dynamics*. 2020;99:919-943.
20. Qatu MS, Iqbal J. Transverse vibration of a two-segment cross-ply composite shafts with a lumped mass. *Composite Structures*. 2010;92:1126-1131.
21. Arab SB, Rodrigues JD, Bouaziz S, Haddar M. Dynamic analysis of laminated rotors using a layerwise theory. *Composite Structures*. 2017;182:335-345.
22. Myklestad NO. A new method of calculating natural modes of coupled bending vibration of airplane wings and other types of beams. *Journal of Aeronautical Science*. 1944;11:153-162.
23. Wu JS, Yang IH. Computer method for torsion and flexure coupled forced vibration of shafting system with damping. *Journal of Sound and Vibration*. 1995;180. (3):417-435.
24. Yang M, Zhou X, Zhang W, Ye J, Hu Y. A modified transfer matrix method for bending vibration of CFRP/Steel composite transmission shafting. *Archive of Applied Mechanics*. 2020;90:603-614.
25. Farshidianfar A, Soheil S, Abachizadeh M. Flexural vibration of Timoshenko beams. using distributed lumped modeling technique. *Aerospace Mechanics Journal*. 2008;4(1):75-84.
26. Soheil S, Abachizadeh M. Flexural vibration of multistep rotating Timoshenko shafts using hybrid modeling and optimization techniques. *Journal of Vibration and Control*. <https://doi.org/10.1177/10775463211072406>; 2022.

Acknowledgements: This paper was inspired by the work carried out under grant RPPK.01.02.00 – 18 – 0029/19 – 00 entitled: "Prace B+R dotyczące innowacyjnej pompy wtryskowej dedykowanej silnikom ciężkich pojazdów i sprzętów o przeznaczeniu specjalnym," co-financed by the European Regional Development Fund.

Stanisław Noga:  <https://orcid.org/0000-0003-3789-4899>

Edward Rejman:  <https://orcid.org/0000-0003-4716-7513>

Paweł Bałon:  <https://orcid.org/0000-0003-3136-7908>

Bartłomiej Kielbasa:  <https://orcid.org/0000-0002-3116-2251>

Robert Smusz:  <https://orcid.org/0000-0001-7369-1162>

Janusz Szostak:  <https://orcid.org/0000-0002-7789-3383>